Electronic Supplementary Material (ESI) for New Journal of Chemistry.
This journal is © The Royal Society of Chemistry and the Centre National de la Recherche Scientifique 2023

Supporting information

Highly Efficient Room-Temperature NO_2 Gas Sensor Based on Three-Dimensional Core-Shell Structured CoS_2 Bridging Co_3O_4@MoS_2.

Haiyang Chang[a,b], Jiahui Fan[b], Kejian Yang[a,*], Cheng Wang[a,b,*], Boxuan Zhang[a], Wanying Zhang[a], Xudong Chen[a,b,*]

a. Key Laboratory of Functional Inorganic Material Chemistry, Ministry of Education. School of Chemistry and Material Science, Heilongjiang University, Harbin, 150080, P. R. China.

b. Guangdong Laboratory of Chemistry and Fine Chemical Engineering Jieyang Center, Jieyang 515200, China E-mail: yang_771172@163.com; wangc_93@gdut.edu.cn; chenxd@gdut.edu.cn

Physical characterization

The phase constituents of the as-products were analyzed by X-ray diffraction (XRD, D/MAX IIB-40KV, Japan) with Cu-K radiation, =1.5406 Å radiation source. The morphology and surface chemical characteristics of the products were observed with a high-resolution transmission electron microscope (TEM, JEOL 2100). The chemical states of the composites were tested using X-ray photoelectron spectrometry measurements (XPS, VGESCALAB MK II using Mg-Ka (1253.6 eV) achromatic X-ray radiation). Binding energies were referenced to the C 1s peak of the (C-C) bond which set at 284.4 eV. The UV-vis diffuse reflectance spectra (DRS) of the samples were tested on a UV-vis spectrophotometer (UV 2550, using $BaSO_4$ for the baseline measurement) with an integrating sphere attachment within the 200-800 nm range. All the electrochemical tests were carried out with a CHI-660E electrochemical workstation (Shanghai Chenhua Instruments Limited, China). Electrochemical impedance spectra (EIS) were carried out under laboratory air conditions. For EIS, a lower voltage amplitude (0.2V) was chosen to reduce sample interference and minimize the signal-to-noise ratio, and the frequency range was set to 1-10^6 Hz. A four-electrode system was used, including a working electrode, counter electrode, reference electrode, and auxiliary electrode. The electrical properties of different samples were studied on the gold interleaved electrode. On the other hand, the three-electrode system was used throughout Mott-Schottky (MS) tests, and it was carried out in a 0.1 M Na_2SO_4 solution. A glass carbon electrode (GCE) covered by the as-fabricated sample was used as a working electrode, a platinum (Pt) plate electrode as a counter electrode, and a saturated calomel electrode as a reference electrode. We indirectly proved the conductivity of the materials themselves by EIS and MS testing. All the electrochemical measurements were carried out at room temperature (23±1°C). The work functions were characterized by Kelvin probe (SKP-5050) at room temperature. Raman spectroscopy (Jobin-Yvon HR 800 micro-Raman spectrometer) is used for molecular structure analysis. Temperature program desorption (TPD) was carried out by AutoChem TP5080 chemisorption analyzer and using mass spectra (QIC-20, Hidden) to record the TPD signals.

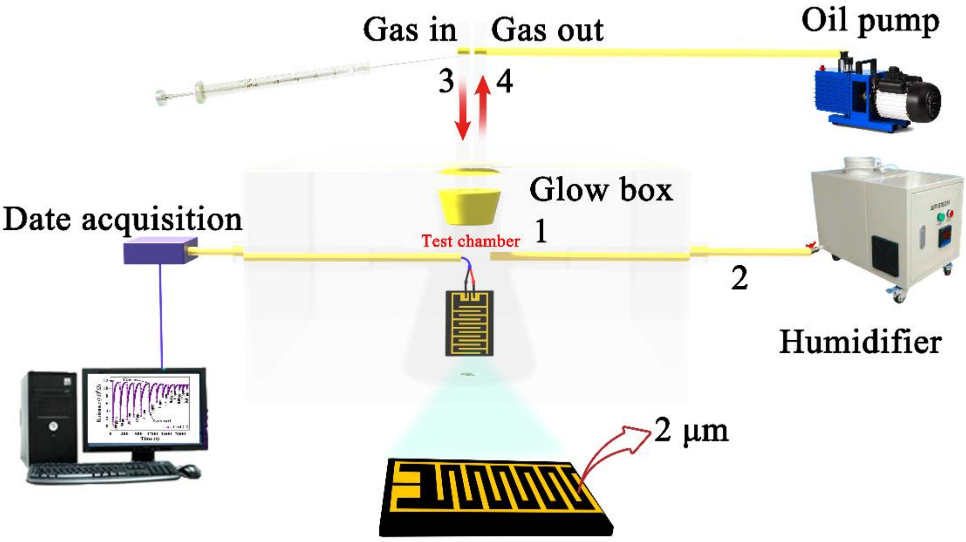

Scheme S1. The gas delivery system diagram for the sensing process.

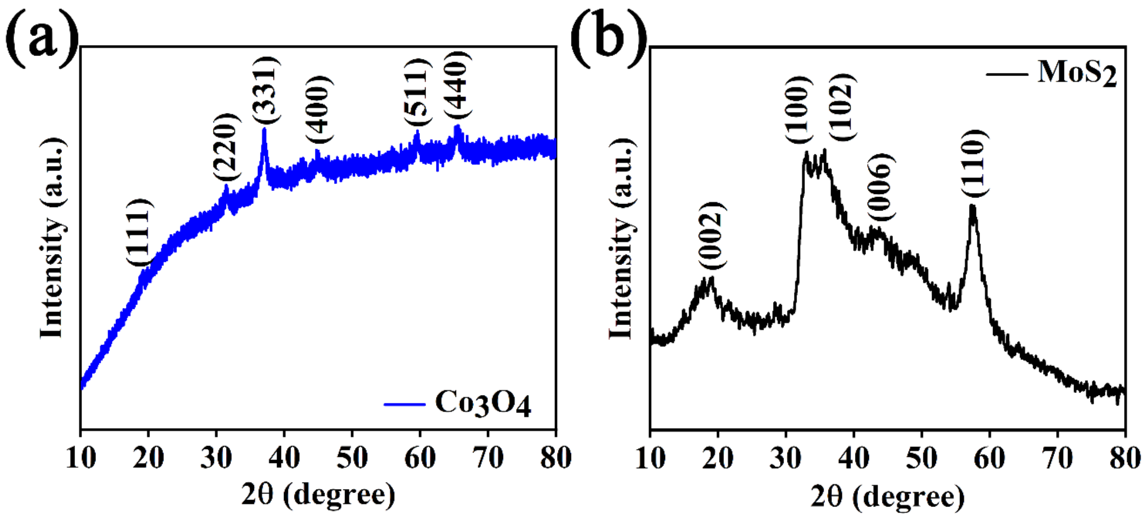

Fig. S1 XRD pattern of the pristine Co_3O_4 and MoS_2.

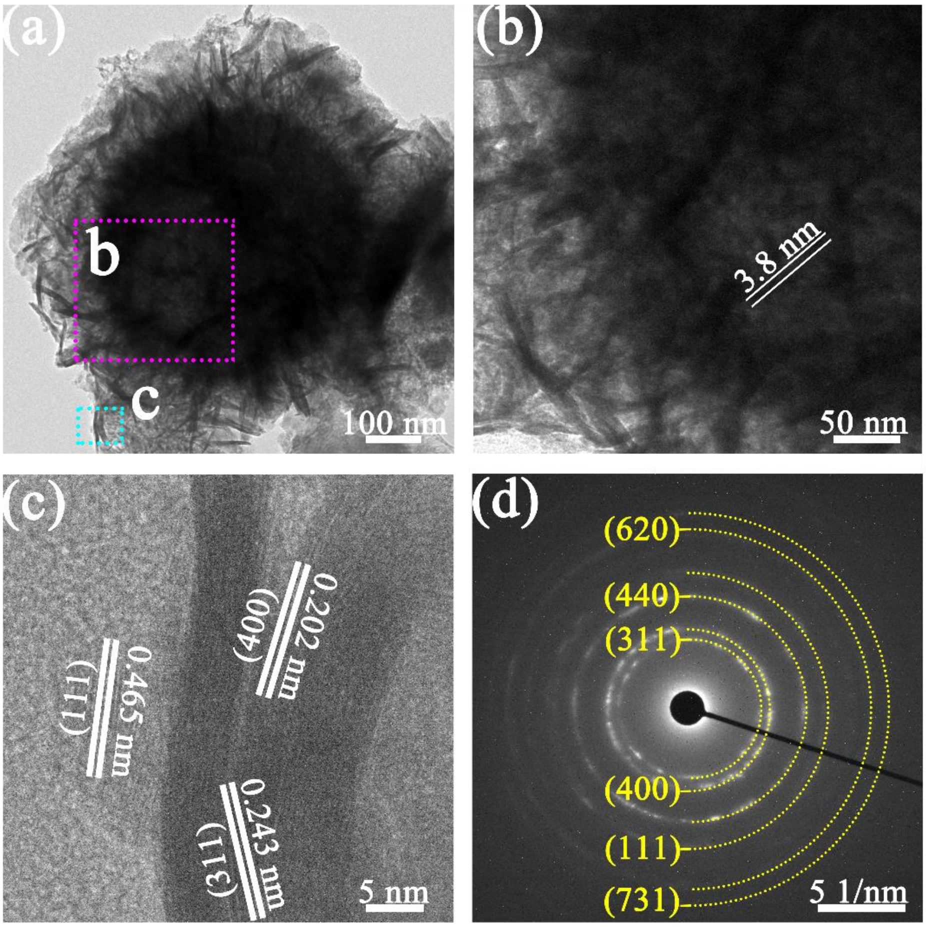

Fig. S2 (a-c) TEM and HRTEM image of pure Co_3O_4, The selected area electron diffraction (SAED) also proved the coexistence of three different crystalline phases in Co_3O_4

Table S1. The comparison of present work on Co_3O_4-CoS_2@MoS_2 with the reported literatures.

Materials	Gas	W. T. (°C)	Gas Conc. (ppm)	T_{res}/T_{rec}	Sensitivity (R_a/R_g)	LOD (ppm)	Ref
This Work	**NO_2**	**RT**	**100**	**3.4s/54.4s**	**39.6**②	**0.01**	**This Work**
Carbon Dots-WO_3	NO_2	RT	5	5s/376s	2.13①	200ppb	[1]
S-doped SnO_2	NO_2	RT	5	27s/32s	10.7②	0.0018	[2]
MoS_2-bilayer	NO_2	RT	10	--	21%①	---	[3]
n-MoS_2/p-GaN	NO_2	RT	50	272s/612s	98.42%①	--	[4]
MoS_2/SnO_2	NO_2	RT	250	--	18.7②	5	[5]
CeO_2-Graphene	NO_2	136	200	250s/2590s	33②	--	[6]
SnS_2/$SnSe_2$	NO_2	RT	2	--	699.2%①	--	[7]
Co_3O_4/rGO	NO_2	RT	5	900s/--	26.8%①	0.05	[8]
n-SnO_2/*p*-Co_3O_4	NO_2	300	10	--	129.8%①	2	[9]
α-Fe_2O_3/Co_3O_4-5 min-rGO	NO_2	130	2	44s/50s	17.64②	0.44ppb	[10]

W.T.: Working temperature; LOD: limit of detection; RT: Room temperature.

①: S=|Ra–Rg|/Ra×100% or S=|Rg–Ra|/Ra×100%

②: S=Ra/Rg

Table S2 Parameters obtained by fitting experimental curve to equivalent circui

Raw materials	R1 (Ω)	C1 (F)	R2 (Ω)	C2 (F)
Co_3O_4-CoS_2@MoS_2-1	1.224×10^{5}	4.712×10^{-11}	1.161×10^{6}	4.534×10^{-10}
Co_3O_4-CoS_2@MoS_2-2	1.276×10^{5}	6.804×10^{-11}	3.248×10^{5}	3.844×10^{-11}
Co_3O_4-CoS_2@MoS_2-3	1.805×10^{5}	1.019×10^{-11}	1.323×10^{6}	2.137×10^{10}
Co_3O_4	3.148×10^{7}	1.045×10^{12}	6.805×10^{7}	3.828×10^{-10}

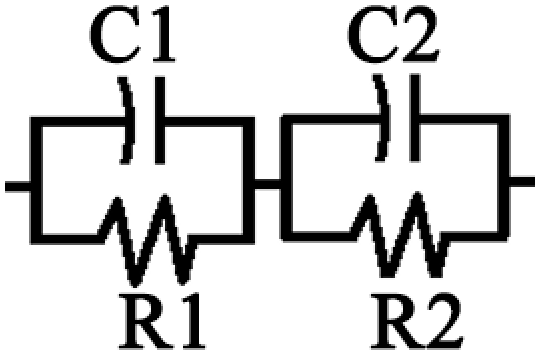

Fig. S3 The equivalent circuit model used to interpret the EIS data

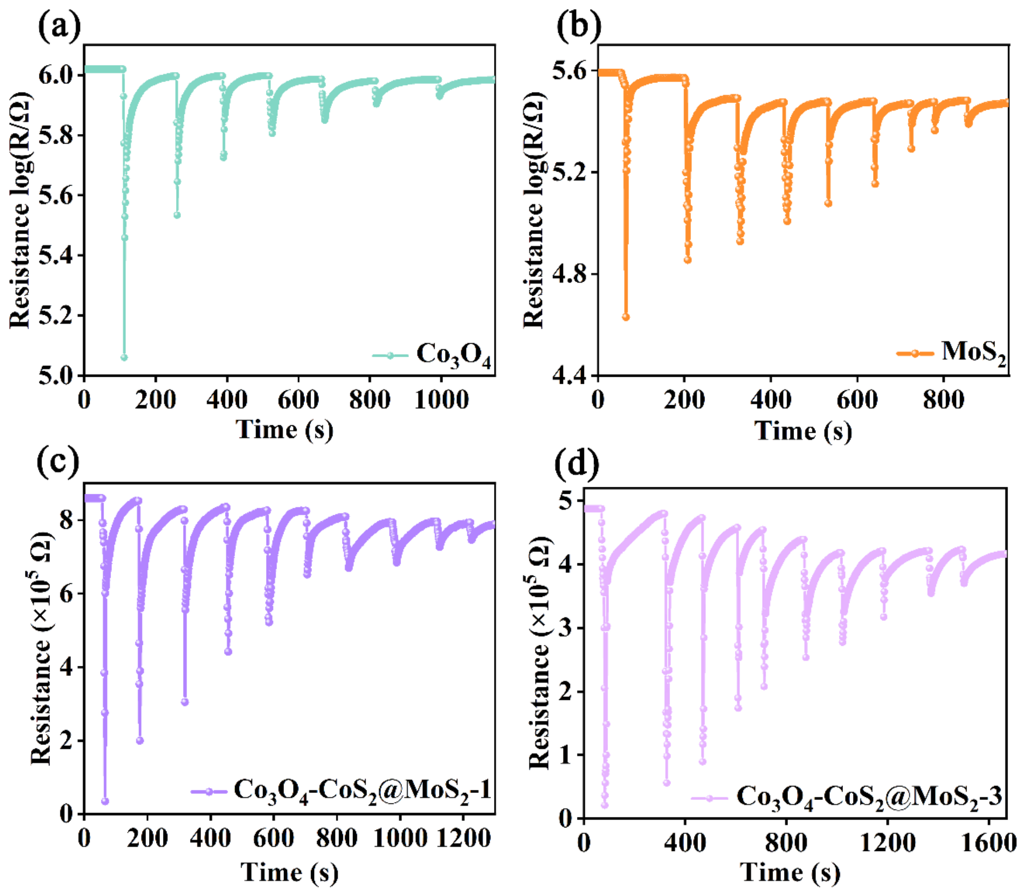

Fig. S4 Dynamic response-recovery time curves of (a) Co_3O_4; (b) Co_3O_4@CoS_2@MoS_2-1; (c) Co_3O_4@CoS_2@MoS_2-3; (d)MoS_2 (RT = 25 ℃, RH= 25 %).

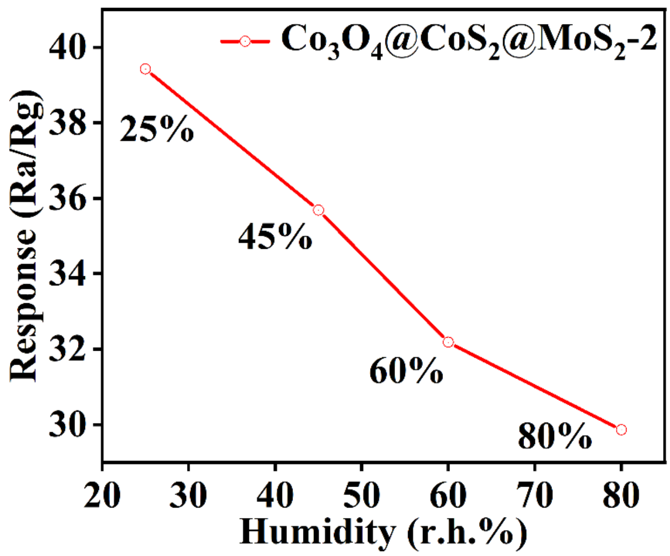

Fig. S5 Response value of Co_3O_4-CoS_2@MoS_2 -2 sensor at different humidity conditions.

Calculation for limit of detection (LOD):

The sensor noise was calculated using the variation in the relative sensor response in the baseline using the root-mean-square deviation (rms). According to the Eq. (1) below, and Si and S obtained by the polynomial fit method in Fig. S10, Vx^2can be gathered as followed [11].

$$Vx^2 = \Sigma(Si - S)^2 \qquad (1)$$

The sensor noise is 0.0003 according to the Eq. (2) and the theoretical detection limit (for signal-to-noise ratio of 3) is approximately 12 ppb according to the Eq. (3).

$$rms = \sqrt{Vx^2/N} \qquad (N = 30) \qquad (2)$$

$$\text{LOD} = 3 * (\text{rms}/\text{slope}) \qquad (3)$$

Therefore, the theoretical detection limit of 1.8 ppb to NO_2 at RT.

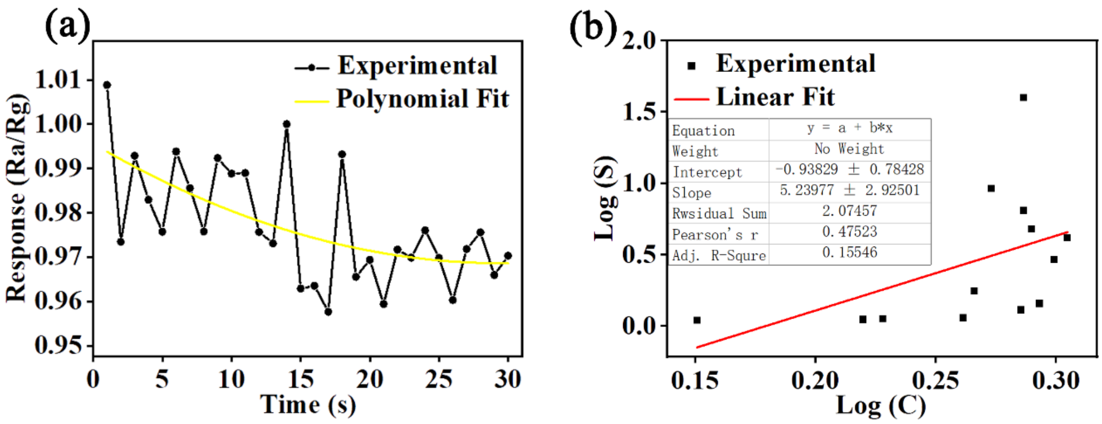

Fig. S6 (a) The curve obtained by fifth-order polynomial fitting the first 30 response points in the response-time baseline of the Co_3O_4-CoS_2@MoS_2-2 sensor before the injection of NO_2. The response values before and after fitting are recorded as Yi and Y, respectively; (b) the curve with detailed data obtained by linear fitting the response points in the NO_2 sensing measurement of Fig. 4a.

Table S3 Response, response time and recovery time of $Co_3O_4@CoS_2@MoS_2$ sensors at room temperature (RT=25 °C, RH 25%).

Sample	**Co_3O_4-$CoS_2@MoS_2$-1**			**Co_3O_4-$CoS_2@MoS_2$-2**			**Co_3O_4-$CoS_2@MoS_2$-3**			**Co_3O_4**		
NO_2(ppm)	**S**	**T/s**	**Tr/s**	**S**	**T/s**	**Tr/s**	**S**	**T/s**	**Tr/s**	**S**	**T/s**	**Tr/s**
100	30.16	7.05	60.04	39.6	3.42	54.40	33.51	6.40	57.32	9.08	9.39	75.87
50	24.27	10.20	55.88	30.21	7.21	50.00	28.55	9.80	54.21	2.90	15.52	67.70
30	22.72	14.37	52.78	26.45	11.20	46.00	25.30	13.38	47.22	1.87	17.94	59.30
10	21.89	18.04	51.56	24.79	15.00	35.60	22.64	17.56	44.20	1.56	29.68	53.54
5	11.58	27.52	49.34	14.16	19.00	24.00	12.19	25.59	31.00	1.37	34.56	41.09
3	10.27	34.00	43.30	12.92	29.40	22.00	11.73	27.94	26.38	1.19	38.98	32.00
1	9.17	38.30	32.04	11.76	35.00	20.00	10.51	37.12	22.00	1.13	41.12	25.00
0.5	7.16	48.33	27.00	10.44	38.00	18.60	8.33	45.00	19.40			
0.3	5.10	50.40	20.67	8.30	40.40	15.00	6.19	49.80	17.30			
0.1	3.06	60.80	18.73	5.14	46.00	10.90	4.14	58.65	15.00			
0.05	1.87	70.87	14.90	3.13	52.20	9.00	2.51	66.32	10.00			
0.03	- -	- -	- -	1.21	56.60	5.60						

*S: Response T_s: Response time T_r: Recovery time

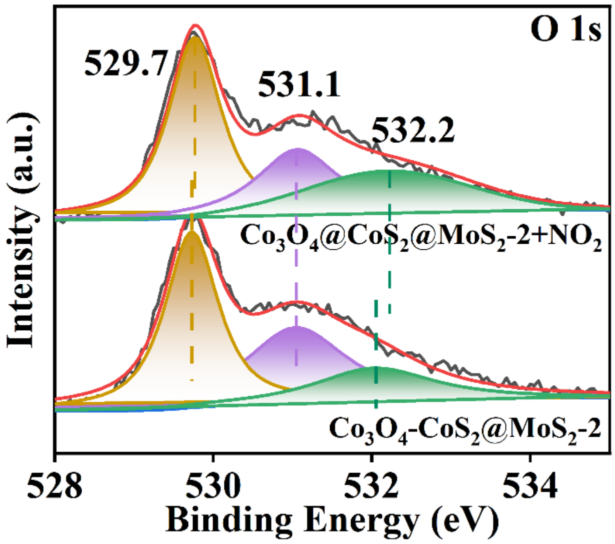

Fig. S7 XPS spectra of Co_3O_4-CoS_2@MoS_2-2 in air and after NO_2 adsorption at RT

Table S4 O1s peak position and peak area ratio (%) of Co_3O_4-CoS_2@MoS_2-2 and Co_3O_4-CoS_2@MoS_2-2+NO_2 samples.

O_l: lattice oxygen; O_V: oxygen vacancy; O_c: chemisorbed oxygen

Sample	Co_3O_4-CoS_2@MoS_2-2			Co_3O_4-CoS_2@MoS_2-2+NO_2		
Peak	O_l	O_V	O_C	O_l	O_V	O_C
Binding energy (eV)	529.73	531.04	532.03	529.76	531.05	532.2
Peak area ratio (%)	49.42	26.29	24.24	45.49	36.45	17.85

Co_3O_4-CoS_2@MoS_2-2+NO_2: Fresh Co_3O_4-CoS_2@MoS_2-2 adsorption NO_2 for 1 h at RT.

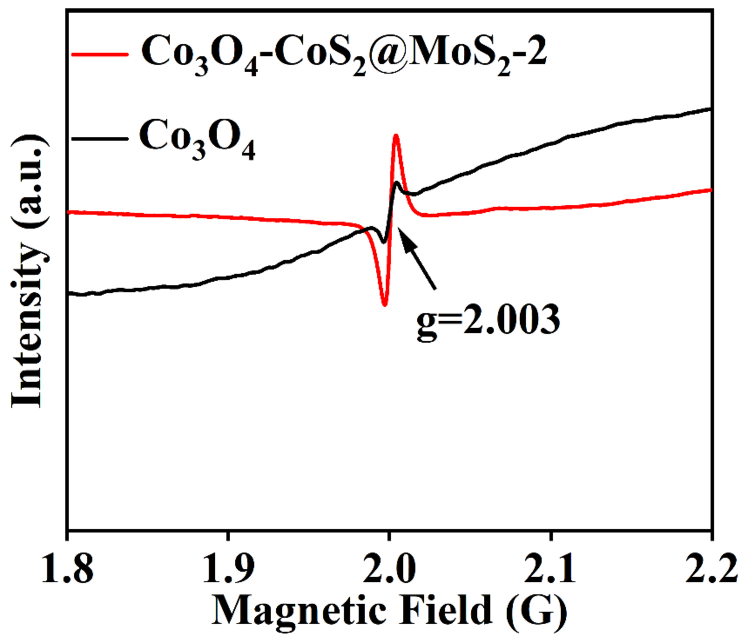

Fig. S8 EPR spectra of Co_3O_4-CoS_2@MoS2-2 and Co_3O_4

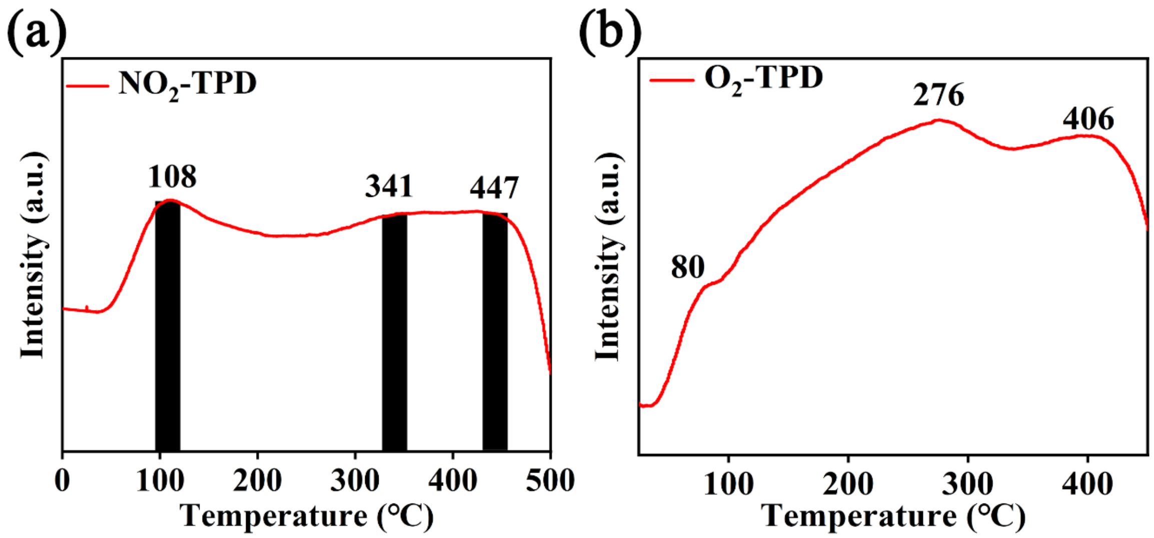

Fig. S9 O_2-TPD and NO_2-TPD of Co_3O_4-CoS_2@MoS_2-2 composite

References

[1] W. Bian, H. Dou, X. Wang, C. Li, Y. Zhang, C. Gong, N. Sun, S. Liu, P. Li, Q. Jing, B. Liu, Fabrication and Computational Study of a Chemiresistive NO_2 Gas Sensor Based on the Carbon Dots-WO_3 Heterostructure for Operating below Room Temperature, ACS Sens, 8 (2023) 748-756.

[2] P. Wang, W. Ge, L. Lin, X. Jia, X. Zhang, J. Lu, S-doped SnO2 derived from SnS nanoparticles for highly sensitive NO2 detection at room temperature, Journal of Alloys and Compounds, 953 (2023).

[3] M. Qi, Z. Huang, H. Zheng, L. Zhao, R. Jiang, J. Wang, J. Hu, G. Chen, S. Jia, J. Wang, Layer-Dependent NO_2-Sensing Performance in MoS2 for Room-Temperature Monitoring, ACS Applied Nano Materials, 6 (2023) 9290-9297.

[4] M. Reddeppa, B.-G. Park, G. Murali, S.H. Choi, N.D. Chinh, D. Kim, W. Yang, M.-D. Kim, NOx gas sensors based on layer-transferred n-MoS2/p-GaN heterojunction at room temperature: Study of UV light illuminations and humidity, Sensors and Actuators B: Chemical, 308 (2020).

[5] Y. Han, Y. Ma, Y. Liu, S. Xu, X. Chen, M. Zeng, N. Hu, Y. Su, Z. Zhou, Z. Yang, Construction of MoS_2/SnO_2 heterostructures for sensitive NO_2 detection at room temperature, Applied Surface Science, 493 (2019) 613-619.

[6] L. Zhang, H. Xu, Y. Huang, H. Lu, T. Ai, K. Xu, F. Ma, P.K. Chu, Polar Cubic CeO_2 Nanoparticles on Graphene for Enhanced Room-Temperature NO_2 Sensing Performance, ACS Applied Nano Materials, 6 (2023) 10551-10558.

[7] R. Wu, K. Yan, J. Zhao, Z. Cai, S. Jian, L. Qiu, 2D/2D SnS_2/$SnSe_2$ van der Waals heterostructure for highly sensitive room-temperature NO_2 sensor: Key role of interface contact, Chemical Engineering Journal, 466 (2023).

[8] B. Zhang, M. Cheng, G. Liu, Y. Gao, L. Zhao, S. Li, Y. Wang, F. Liu, X. Liang, T. Zhang, G. Lu, Room temperature NO_2 gas sensor based on porous Co_3O_4 slices/reduced graphene oxide hybrid, Sensors and Actuators B: Chemical, 263 (2018) 387-399.

[9] Y.J. Kwon, H.G. Na, S.Y. Kang, M.S. Choi, J.H. Bang, T.W. Kim, A. Mirzaei, H.W. Kim, Attachment of Co_3O_4 layer to SnO_2 nanowires for enhanced gas sensing properties, Sensors and Actuators B: Chemical, 239 (2017) 180-192.

[10] L. Sun, J. Sun, K. Zhang, X. Sun, S. Bai, Y. Zhao, R. Luo, D. Li, A. Chen, rGO functionalized α-Fe_2O_3/Co_3O_4 heterojunction for NO_2 detection, Sensors and Actuators B: Chemical, 354 (2022).

[11] J. Fan, L. Jiang, H. Lv, F. Qin, Y. Fan, J. Wang, M. Ikram, K. Shi, ZIF-67/BiOCl nanocomposites for highly efficient detection of NO_2 gas at room temperature, Journal of Materials Chemistry A, 11 (2023) 15370-15379.